



Brazilian Journal of Physics

ISSN: 0103-9733

luizno.bjp@gmail.com

Sociedade Brasileira de Física

Brasil

Avancini, S. S.; Menezes, D. P.; Brito, L.; Providência, C.  
Asymmetric Nuclear Matter and its Instabilities  
Brazilian Journal of Physics, vol. 35, núm. 3B, september, 2005, pp. 832-834  
Sociedade Brasileira de Física  
São Paulo, Brasil

Available in: <http://www.redalyc.org/articulo.oa?id=46435531>

- How to cite
- Complete issue
- More information about this article
- Journal's homepage in redalyc.org

redalyc.org

Scientific Information System  
Network of Scientific Journals from Latin America, the Caribbean, Spain and Portugal  
Non-profit academic project, developed under the open access initiative

## Asymmetric Nuclear Matter and its Instabilities

S. S. Avancini, D. P. Menezes,

Depto de Física - CFM - Universidade Federal de Santa Catarina - Florianópolis - SC - CP. 476 - CEP 88.040 - 900 - Brazil

L. Brito, and C. Providência

Centro de Física Teórica - Depto de Física - Universidade de Coimbra - 3000 - Portugal

Received on 31 May, 2005

In order to investigate the instabilities in asymmetric nuclear matter described within relativistic mean field hadron models, we build the spinodals. We have used relativistic models both with constant and density dependent couplings at zero and finite temperatures. We have seen that the main differences in the spinodals occur at finite temperature and large isospin asymmetry close to the boundary of the instability regions.

It is important to test the relativistic models often used in the literature at finite temperature and different densities, since these models can describe the ground state of both stable and unstable nuclei [1] as well as the properties of neutron stars and supernovae [2], once the couplings are conveniently adjusted.

Asymmetric nuclear matter (ANM) may present instabilities and phase transitions. This is a topic of great interest nowadays. The instabilities present in ANM may manifest themselves as an isospin distillation or fractionation [3]. Multifragmentation also takes place when the system enters the spinodal region through nucleation or through spinodal decomposition. The correlation between spinodal decomposition and negative heat capacity evidences the fact that the spinodal decomposition is the dynamics underlying the liquid gas phase transition [4]. Also in neutron stars the underlying asymmetry of the equation of state which is used to describe it is an important source of investigation. It has recently been proposed that there is a relationship between the neutron skin of heavy nuclei and the properties of neutron star crusts, namely the thicker the neutron skin of a heavy nucleus the thinner the solid crust of a neutron star.

Moreover, standard relativistic mean field interactions show limitations for describing nuclei close to the stability line. This is due to the fact that the isovector channel is poorly constrained by experimental data. An example is the systematic overestimate of the neutron skins [5]. Some of these limitations are overcome by quantum hydrodynamical models with density dependent meson-nucleon couplings (which we refer to as TW) [6, 7], which have been used with success to describe both nuclear matter and finite nuclei.

We may ask whether the recent improvements of the RMF models, both through the inclusion of density dependent meson-nucleon couplings and/or the  $\delta$  scalar-isovector meson, present different features at subnuclear densities of nuclear asymmetric matter which could have consequences for the properties of the inner crust of neutron stars or in multifragmentation or isospin fractionation reactions. The parametrizations of these models take generally into account saturation properties of nuclear matter and properties of stable nuclei. Extension of the model for very asymmetric nuclear matter or to finite temperatures may show different behaviors. The simplest test between the models is a comparison of the

regions of uniform unstable matter.

We start from the lagrangian density of the relativistic TW model [6]

$$\begin{aligned} \mathcal{L} = & \bar{\Psi} \left[ \gamma_\mu \left( i\partial^\mu - \Gamma_\nu V^\mu - \frac{\Gamma_\rho}{2} \vec{\tau} \cdot \vec{b}^\mu \right) - (M - \Gamma_s \phi) \right] \Psi \\ & + \frac{1}{2} (\partial_\mu \phi \partial^\mu \phi - m_s^2 \phi^2) - \frac{1}{4} \Omega_{\mu\nu} \Omega^{\mu\nu} + \frac{1}{2} m_\nu^2 V_\mu V^\mu \\ & - \frac{1}{4} \vec{B}_{\mu\nu} \cdot \vec{B}^{\mu\nu} + \frac{1}{2} m_\rho^2 \vec{b}_\mu \cdot \vec{b}^\mu, \end{aligned} \quad (1)$$

where  $\Omega_{\mu\nu} = \partial_\mu V_\nu - \partial_\nu V_\mu$ ,  $\vec{B}_{\mu\nu} = \partial_\mu \vec{b}_\nu - \partial_\nu \vec{b}_\mu - \Gamma_\rho (\vec{b}_\mu \times \vec{b}_\nu)$ . The parameters of the model are: the nucleon mass  $M = 939$  MeV, the masses of the mesons  $m_s$ ,  $m_\nu$ ,  $m_\rho$ , and the density dependent coupling constants  $\Gamma_s$ ,  $\Gamma_\nu$  and  $\Gamma_\rho$ , which are adjusted in order to reproduce some of the nuclear matter bulk properties[6].

Other possibilities for these parameters are also found in the literature [8]. Notice that in this model the non-linear terms are not present in eq.(1), in contrast with the usual non-linear Walecka model (NLWM). The equations of motion are then obtained in a mean field approximation and the distribution function reads  $f_{i\pm} = 1/\{1 + \exp[(E^* \mp v_i)/T]\}$ , where the effective chemical potential is  $v_i = \mu_i - \Gamma_\nu V_0 - \tau_{i3} \frac{\Gamma_\rho}{2} b_0 - \Sigma_0^R$ ,  $\tau_{p3} = 1$ ,  $\tau_{n3} = -1$ , with the rearrangement term given by

$$\Sigma_0^R = \frac{\partial \Gamma_\nu}{\partial \rho} \rho V_0 + \frac{\partial \Gamma_\rho}{\partial \rho} \rho_3 \frac{b_0}{2} - \frac{\partial \Gamma_s}{\partial \rho} \rho_s \phi_0. \quad (2)$$

The energy density in the mean field approximation reads:

$$\begin{aligned} \mathcal{E}(\Gamma_s, \Gamma_\nu, \Gamma_\rho) = & 2 \sum_i \int \frac{d^3 p}{(2\pi)^3} E^* (f_{i+} + f_{i-}) \\ & + \frac{m_s^2}{2} \phi_0^2 + \frac{m_\nu^2}{2} V_0^2 + \frac{m_\rho^2}{2} b_0^2. \end{aligned} \quad (3)$$

and the pressure becomes

TABLE I: Nuclear matter properties.

	NL3 [9]	TM1 [10]	TW [6]	NL $\delta$ [11]	DDH $\rho\delta$ [12]
$B/A$ (MeV)	16.3	16.3	16.3	16.0	16.3
$\rho_0$ (fm $^{-3}$ )	0.148	0.145	0.153	0.160	0.153
$K$ (MeV)	272	281	240	240	240
$E_{\text{sym}}$ (MeV)	37.4	36.9	32.0	30.5	25.1
$M^*/M$	0.60	0.63	0.56	0.60	0.56

$$P(\Gamma_s, \Gamma_v, \Gamma_\rho) = \frac{1}{3\pi^2} \sum_i \int dp \frac{\mathbf{p}^4}{E^*} (f_{i+} + f_{i-}) - \frac{m_s^2}{2} \phi_0^2 + \frac{m_v^2}{2} V_0^2 + \frac{m_\rho^2}{2} b_0^2 - \rho \Sigma_0^R. \quad (4)$$

For two of the usual NLWM parametrizations, namely NL3 [9] and TM1 [10], the above equations read:

$$\begin{aligned} \mathcal{E} &= \mathcal{E}(g_s, g_v, g_\rho) + \frac{\kappa \phi_0^3}{6} + \frac{\lambda \phi_0^4}{24} + \frac{\xi g_v^4 V_0^4}{8}, \\ P &= P(g_s, g_v, g_\rho) - \frac{\kappa \phi_0^3}{6} - \frac{\lambda \phi_0^4}{24} + \frac{\xi g_v^4 V_0^4}{24}, \end{aligned} \quad (5)$$

where the meson-nucleon coupling constants,  $g_s, g_v$ , and  $g_\rho$  substitute  $\Gamma_s, \Gamma_v$ , and  $\Gamma_\rho$ . They are not density dependent and consequently all derivative terms in the pressure cancel out and  $\kappa, \lambda$  and  $\xi$  are the self-coupling constants multiplying the non-linear terms.

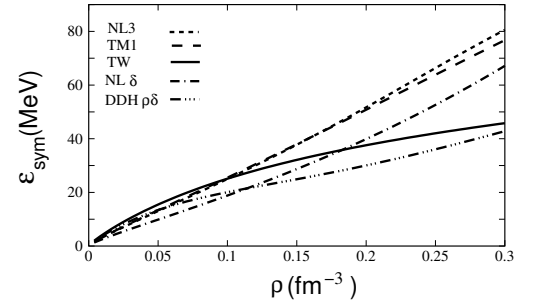
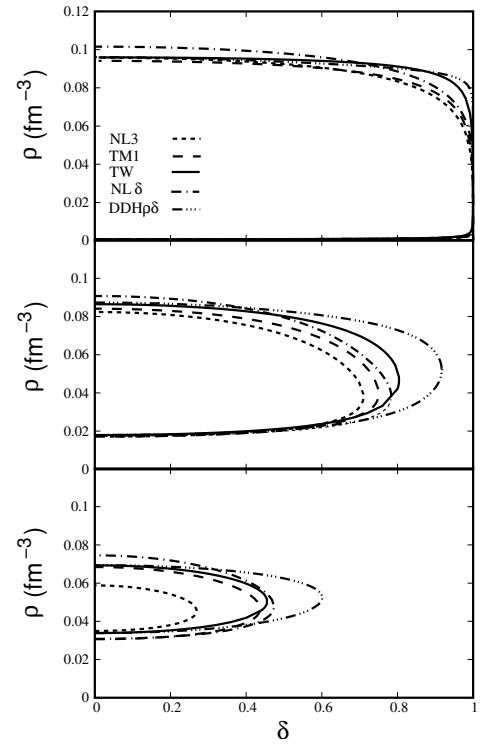
To investigate the influence of the  $\delta$ -meson in the stability conditions we have included in both the density dependent and the NLWM models, the isovector-scalar meson terms [11]:

$$\mathcal{L} = g_\delta \bar{\psi} \vec{\tau} \cdot \vec{\delta} \psi + \frac{1}{2} (\partial_\mu \vec{\delta} \partial^\mu \vec{\delta} - m_\delta^2 \vec{\delta}^2), \quad (6)$$

where  $g_\delta$  and  $m_\delta$  are respectively the coupling constant of the  $\delta$  meson with the nucleons and its mass. Self-interacting terms for the  $\sigma$ -meson are also included,  $\kappa$  and  $\lambda$  denoting the corresponding coupling constants.

For reference, in Table I we show the properties of nuclear matter reproduced by the models we discuss in the present work. The equation of motion for this field becomes  $\delta_3 = \frac{g_\delta}{m_\delta^2} \rho_{s3}$ , with  $\rho_{s3} = \rho_{sp} - \rho_{sn}$ . The energy density and the pressure are also affected by the presence of the new meson. The term  $+1/2 m_\delta^2 \delta_3^2$  should be added to the energy density and the  $-1/2 m_\delta^2 \delta_3^2$  should be added to the expression of the pressure, both given in eq. (5). The effective masses for protons and neutrons acquire different values, namely,

$$M_i^* = M - g_s \phi_0 - \tau_{i3} g_\delta \delta_3 \quad i = p, n.$$

FIG. 1: Symmetry energy results for the NL3, TM1, TW, NL $\delta$  and DDH $\rho\delta$  parameter sets.FIG. 2: Spinodal regions for different parameter sets and  $T = 0$  (upper panel),  $T = 10$  MeV (middle panel) and  $T = 14$  MeV (lower panel).

For completeness, we have also included the  $\delta$ -meson in a model where the  $\rho$  and  $\delta$  couplings are density dependent, as done in [12], where it is called density dependent hadronic model (DDH $\rho\delta$ ). In this case the coupling constants  $g_s, g_v, g_\rho$  and  $g_\delta$  used in equation (6) should be replaced by  $\Gamma_s, \Gamma_v, \Gamma_\rho$  and  $\Gamma_\delta$  and the non-linear scalar terms do not appear. The rearrangement term appearing in the effective chemical potential and pressure now has the extra term  $-\frac{\partial \Gamma_\delta}{\partial \rho} \rho_{s3} \delta_3$  and the pressure becomes  $P(\Gamma_s, \Gamma_v, \Gamma_\rho, \Gamma_\delta) = P(\Gamma_s, \Gamma_v, \Gamma_\rho) - \frac{m_\delta^2}{2} \delta_3^2$ .

The stability conditions for asymmetric nuclear matter in

terms of the proton fraction read

$$\left(\frac{\partial P}{\partial \rho}\right)_{T,y_p} > 0, \quad \text{and} \quad \left(\frac{\partial P}{\partial \rho}\right)_{T,y_p} \left(\frac{\partial \mu_p}{\partial y_p}\right)_{T,P} > 0. \quad (7)$$

It has recently been argued [13, 14] that in ANM the spinodal instabilities cannot be separately classified as mechanical or chemical instabilities. In fact, the two mentioned conditions in equation (7) that give rise to the instability of the system are coupled so that it appears as a mixture of baryon density and concentration fluctuations.

In order to calculate the boundaries of the spinodal instability regions we use the well known Gibbs-Duhem relation, at a fixed temperature and isospin asymmetry with  $\delta = -\rho_3/\rho = 1 - 2y_p$  [15]. The spinodal regions can then be obtained for both different temperatures and different parametrizations.

A quantity of interest in ANM is the nuclear bulk symmetry energy discussed in [16]. This quantity is important in studies involving neutron stars and radioactive nuclei. The behavior of the symmetry energy at densities larger than nuclear saturation density is still not well established. In general, relativistic and non-relativistic models give different predictions for the symmetry energy. It is usually defined as  $E_{\text{sym}} = \frac{1}{2} \frac{\partial^2 E/\rho}{\partial \delta^2} \Big|_{\delta=0}$ .

In Fig.1 we show the symmetry energy for the different models used in this work, calculated at  $T = 0$  and  $y_p = 0.5$ . We can see that at subsaturation densities where the instability regions occur (0 up to  $0.1 \text{ fm}^{-3}$ ), NL3 and TM1 parametrizations give very similar behaviors. The NL $\delta$  parametrization describes saturation at  $0.16 \text{ fm}^{-3}$  and this fact affects the symmetry energy at low densities, in particular it is the model with the lowest symmetry energy in this range of densities (see Table I). The TW model presents a different behavior, after a faster increase at low densities, the symmetry energy increases much slower than most of the other models at larger densities. A very low value of the symmetry energy was obtained with the DDHp $\delta$  parametrization. It amounts to 25 MeV. The density dependent hadronic models show a softer symmetry energy at the densities shown. At higher densities the models containing the  $\delta$ -meson are expected to get a harder behavi-

our due to relativistic effects, namely the  $\delta$  contribution goes to zero and only the repulsive contribution from the  $\rho$ -meson remains [11].

In Fig. 2 we display the spinodals for different parameter sets obtained with  $T = 0, 10, 14 \text{ MeV}$ . For  $T = 0 \text{ MeV}$  the differences are not significant, occurring at the higher density branch,  $\sim 0.1 \text{ fm}^{-3}$ . In particular, in the NL $\delta$  parametrization the boundary lies at a larger density than in the other models for  $\delta < 0.5$ . The spinodals for the density dependent hadronic models are decreasing less with the asymmetry parameter  $\delta$  than the others. At finite temperature the differences are larger. These differences occur again in the larger density branch, and it is again the NL $\delta$  which presents a boundary at larger densities in the small asymmetry region followed by the TW and the DDHp $\delta$  models. In the large asymmetry region we are already testing both the critical temperatures and asymmetries of the models and the differences between the models are larger. For the DDHp $\delta$  model, as temperature increases, the instability boundaries extend to higher asymmetries as compared with all the other models. This is possibly due to a lower symmetry energy. The opposite occurs with the NL3 parametrization which has the larger symmetry energy. We conclude that the information obtained from the spinodal decomposition sensitive to the underlying model comes from the phase space close to the spinodal boundary at large isospin asymmetry.

In conclusion, we have compared the spinodal boundary as a function of density and isospin asymmetry, at several temperatures, for different relativistic models. We have considered both quantum hadrodynamical approaches with non-linear terms (NL3, TM1, NL $\delta$ ) and density dependent hadronic models with density dependent coupling parameters (TW, DDHp $\delta$ ). The largest differences between the models occur at finite temperature and are more clearly shown in the high isospin asymmetry region.

This work was partially supported by CNPq (Brazil), CAPES(Brazil)/GRICES (Portugal) under project 100/03 and FEDER/FCT (Portugal) under the project POCTI /35308/FIS/ 2000.

- 
- [1] P.-G. Reinhard, M. Rufa, J. Maruhn, W. Greiner and J. Friedrich, Z. Phys. A **323**, 13 (1986); Y. Sugahara and H. Toki, Nucl. Phys. A **579**, 557 (1994).
  - [2] H. Shen, H. Toki, K. Oyamatsu and K. Sumiyoshi, Nucl. Phys. A **637**, 435 (1998); D.P. Menezes and C. Providência, Phys. Rev. C **68**, 035804 (2003); P.K. Panda, D.P. Menezes and C. Providência, Phys. Rev. C **69** 025207 (2004); D.P. Menezes and C. Providência, Phys. Rev. C **69** 045801 (2004).
  - [3] H. S. Xu, *et al*, Phys. Rev. Lett. **85**, 716 (2000).
  - [4] B. Borderie *et al.*, nucl-exp/0311016.
  - [5] B. Alex Brown, Phys. Rev. Lett. **85**, 5296 (2000).
  - [6] S. Typel and H. H. Wolter, Nucl. Phys. A **656**, 331 (1999).
  - [7] S.S. Avancini, M.E. Bracco, M. Chiapparini and D.P. Menezes, Phys. Rev. C **67**, 024301 (2003); S.S. Avancini, M.E. Bracco, M. Chiapparini and D.P. Menezes, J. Phys. G **30**, 27 (2004).
  - [8] G. Hua, L.Bo and M. Di Toro, Phys. Rev. C **62**, 035203 (2000).
  - [9] G. A. Lalazissis, J. König and P. Ring, Phys. Rev. C **55**, 540 (1997).
  - [10] K. Sumiyoshi, H. Kuwabara, H. Toki, Nucl. Phys. A **581**, 725 (1995).
  - [11] B. Liu, V. Greco, V. Baran, M. Colonna and M. Di Toro, Phys. Rev. C **65**, 045201 (2002).
  - [12] T. Gaitanos, M. Di Toro, S. Typel, V. Baran, C. Fuchs, V. Greco and H. H. Wolter, Nucl. Phys. A **732**, 24 (2004).
  - [13] V. Baran, M. Colonna, M. Di Toro, and V. Greco, Phys. Rev. Lett. **86**, 4492 (2001).
  - [14] J. Margueron and P. Chomaz, Phys. Rev. C **67**, 041602 (2003).
  - [15] S.S. Avancini, L. Brito, D.P. Menezes and C. Providência, Phys. Rev. C **70**, 015203 (2004).
  - [16] B.-A. Li, C. M. Ko and W. Bauer, Int. J. Mod. Phys. E **7** (1997) 147.